Available online at www.sciencedirect.com
SCIENCE DIRECT®
Journal of Photochemistry and Photobiology A: Chemistry 160 (2003) 185–194
Journal of Photochemistry and Photobiology A:Chemistry
www.elsevier.com/locate/jphotochem

Thick titanium dioxide films for semiconductor photocatalysis

Andrew Mills [a,*], George Hill [a], Sharan Bhopal [a], Ivan P. Parkin [b], Shane A. O'Neill [b]

[a] *Department of Pure and Applied Chemistry, University of Strathclyde, Thomas Graham Building, 295 Cathedral Street, Glasgow G1 1XL, UK*
[b] *Christopher Ingold Laboratory, Department of Chemistry, University College London, 20 Gordon Street, London WCIH OAJ, UK*

Received 31 March 2003; accepted 22 April 2003

Abstract

Thick paste TiO_2 films are prepared and tested for photocatalytic and photoinduced superhydrophilic (PSH) activity. The films are effective photocatalysts for the destruction of stearic acid using near or far UV and all the sol–gel films tested exhibited a quantum yield for this process of typically 0.15%. These quantum yields are significantly greater (4–8-fold) than those for titania films produced by an APCVD technique, including the commercial self-cleaning glass product Activ™. The films are mechanically robust and optically clear and, as photocatalysts for stearic acid removal, are photochemically stable and reproducible. The kinetics of stearic acid photomineralisation are zero order with an activation energy of ca. 2.5 kJ mol^{-1}. All titania films tested, including those produced by APCVD, exhibit PSH. The light-induced fall, and dark recovery, in the water droplet contact angle made with titania paste films are similar in profile shape to those described by others for thin titania films produced by a traditional sol–gel route.

Keywords: Titanium dioxide; Sol–gel film; APCVD technique; Photocatalysis

1. Introduction

Semiconductor photocatalysis offers convenient routes to the purification of air and water and the provision of self-maintaining clean surfaces [1,2]. Semiconductor photocatalysis is based on the feature that some semiconductors, in particular titanium dioxide, are able to photocatalyse the complete mineralisation of many organics, including: aromatics, halohydrocarbons, insecticides, pesticides, dyes, hormones and surfactants. The overall process can be summarised as follows:

$$\text{organic pollutant} + O_2 \xrightarrow[\text{semiconductor}]{h\nu \geq E_{bg}} \text{mineralized products} \quad (1)$$

where E_{bg} is the bandgap of the semiconductor [1,2].

This area of research is dominated by the use of titanium dioxide as the semiconductor photocatalyst since it is biologically and chemically inert, usually very photoactive, readily available and cheap. In the early days of this research the titanium dioxide was used in the form of powder particles, either dispersed in solution or weakly bound to some inert substrate such as glass, or glass fibre. As such systems have developed, and neared, or reached, commercialisation, it has become increasingly clear that the more practical form of the semiconductor photocatalyst is as a film, strongly bound to an inert substrate such as glass or ceramic [3]. Indeed, several major glass manufacturers, including Pilkington Glass and the Pittsburgh Plate Company, have recently released self-cleaning glass products (Activ™ and Sunclean™, respectively) which utilise, as their common active ingredient, a thin, strongly bound, nanocrystalline film of titania that acts as a photocatalyst, for the mineralisation of surface-deposited or gaseous organic pollutants by oxygen, that deposit onto the surface of the glass [3].

In addition to its ability to photodegrade organic contaminants via reaction (1), UV irradiation of titania has been found to induce a patchwork of superhydrophilicity across the surface, i.e. photoinduced superhydrophilicity, or PSH [2,4,5]. This property of PSH, along with its semiconductor photocatalytic activity, is maintained by the UV component of sunlight so that any contaminants on the surface will either be photomineralised or readily washed away by rain water. The phenomenon of PSH involves the trapping of photogenerated holes at lattice, usually bridging, oxygen sites at, or close to, the surface of the semiconductor. Such trapped holes weaken the bond between the associated titanium and the lattice oxygen, allowing the oxygen to be liberated, thus creating an oxygen vacancy. The subsequent dissociative adsorption of water at the site renders it more hydroxylated and, since this process is repeated to lesser and greater extents, depending upon the density of surface

* Corresponding author.
E-mail address: a.mills@strath.ac.uk (A. Mills).

1010-6030/$ – see front matter © 2003 Elsevier Science B.V. All rights reserved.
doi:10.1016/S1010-6030(03)00206-5

bridging oxygen groups, across the illuminated surface of the titania, the result is the photogeneration of a patchwork quilt of hydrophilic domains (typically 10 nm in size) [4]. Such a surface is not stable however, and over some time (typically days), in the dark the photogenerated weakly bound hydroxyl groups reactively desorb in a manner that returns the surface to its original, more hydrophobic form. In PSH the photogenerated electrons are assumed to be trapped by Ti(IV) sites, thus generating Ti(III) species which are subsequently oxidised by oxygen. The overall process can be summarised by the following reaction equation:

$$\equiv\text{Ti–O–Ti}\equiv + \text{H}_2\text{O} \underset{\text{dark},\Delta,k_{-2}}{\overset{h\nu\geq E_{\text{bg}},k_2}{\rightleftarrows}} \equiv\text{Ti–OH HO–Ti}\equiv \qquad (2)$$

where k_2 and k_{-2} are the hydrophilic conversion rate constants for the forward and reverse processes. There are many different methods of preparing thin, usually nanocrystalline, films of titanium dioxide including: CVD, sputtering and thermal oxidation. However, the simplest and most popular approach centres on a sol–gel method involving, typically, the controlled hydrolysis of titanium(IV) isopropoxide to form an hydroxylated form of titanium(IV) that can be coated onto an inert substrate, such as glass, by dipping or spinning [6,7]. In order to complete the process and produce a hard, robust coat of titanium dioxide on the substrate the coated substrate is then usually subjected to a high temperature annealing process, typically 450 °C for 30 min.

The sol–gel solutions that are used to produce such titanium dioxide sol–gel films are usually non-viscous and as a consequence the final films are often very thin, i.e. less than 100 nm and have low absorbances (less than 0.1) in the near-UV region, i.e. $320 > \lambda > 380$ nm, but high absorbances in the far UV, i.e. $\lambda < 280$ nm [6–8]. However, most of the UV component of sunlight falls in the near-UV region and, although cheap, far-UV sources are readily available, such as germicidal fluorescent tubes which emit almost exclusively at 254 nm, in practice their general use is undesirable as far-UV causes substantial damage to most biological systems and can cause cancer. Cheap, efficient, artificial near-UV sources are also available, such as the ubiquitous fluorescent black light bulb (BLB). These lamps are long lasting (typically >3000 h) and emit a broad band (±20 nm) of near-UV light centred at 365 nm. It follows from the above discussion that the main problem with utilising efficiently near-UV light, either from sunlight or BLBs using titanium dioxide as the semiconductor photocatalyst, is that the coating would have to be thick, i.e. typically >1 μm, as well as exhibiting the usual desired features of any coating, i.e. clarity, mechanical robustness, and, of course, high photoactivity.

It is possible to make thick titania films from the typical non-viscous sol–gel solutions referred to above using a repeat "coat and bake" process until the desired thickness is achieved [5,8]. However, such a procedure often produces final films that are cracked and fragile as an appreciable number cycles (>10) are usually required. In a recent paper, a method of producing thick (>1 μm) films of titania was described and the photocatalytic properties of such films reported briefly [9]. In this paper, the results of a more detailed investigation of the photocatalytic and PSH properties of these thick titania films are described and compared with those produced by a traditional sol–gel coating process and by an atmospheric pressure chemical vapour deposition, i.e. APCVD, technique; the latter is currently the preferred method of production of commercial forms of titanium dioxide coated glass.

2. Experimental

2.1. Materials and methods

Unless stated otherwise all chemicals were purchased from Aldrich Chemicals (UK) and used as received. UV-Vis absorption spectra were recorded using a Lambda 20 UV-Vis spectrophotometer (Perkin Elmer, UK). Contact angles were measured using an FTA 200 contact angle instrument (supplied by Camtel, UK), details of which are described elsewhere [10]. In brief, the system allows CCTV images of the water droplets on the test substrate to be recorded and then used to calculate the contact angles the droplets make on the test substrate. All contact angles reported in this paper refer to water droplets 30 s after the drop has made contact with the substrate under test. In demonstrating the PSH action of the titania-coated, and non-coated, glass substrates, ultra-bandgap irradiation of the films was carried out using two 8 W 254 nm germicidal lamps (BDH, UK).

In the study of the photocatalytic activities of the various titanium dioxide films, stearic acid was used as the test organic material for mineralisation. Stearic acid was chosen as it provides a good representation of the organic solid films that deposit on window glass and because it is very readily deposited to create films that are easily analysed by transmission FT-IR. Each film under test was coated with an initial layer of stearic acid by dropping 0.3 cm^3 of a stearic acid in chloroform solution (30 g dm^{-3}) onto the surface of the film and then spinning it at 500 rpm for 10 s. Each film was then placed in an oven at 393 K for 30 s and then allowed to cool to room temperature. A 1600 FT-IR (Perkin Elmer, UK) was used to record the FT-IR spectra and calculate the integrated area under the stearic acid peaks over the range 2500–3500 cm^{-1}, from which the concentration of stearic acid was calculated [7,10]. Thus FT-IR transmission spectroscopy allowed the concentration of stearic acid on a test substrate to be measured (in units of molecules of stearic acid cm^{-2}) and monitored as a function of irradiation time.

In the study of the photocatalytic activities of the various films the irradiation source was either six 8 W BLBs or six 8 W germicidal lamps, each set in a half cylinder unit, with a backing aluminium reflector. In either case the sample

under test was placed on the bench and the irradiation unit placed 13 cm vertically above it. The light outputs for the two illumination sources, i.e. the BLB and germicidal lamps, were determined by ferrioxalate actinometry [11] to be 7.6×10^{17} and 4.6×10^{17} photon cm^{-2} min^{-1}, respectively.

2.2. Preparation of the thick titanium dioxide films

The preparation of the thick titanium dioxide films is described in detail elsewhere [9]. Briefly 4.65 g of acetic acid were added to 20 ml of titanium isopropoxide under an inert nitrogen atmosphere. To this were added 120 ml of 0.1 mol dm^{-3} nitric acid and, after mixing the reaction solution, was heated rapidly to 80 °C whereupon it turned milky white and opaque. Within a few minutes at this temperature the reaction solution gelled but became fluid again within 1–2 h. The reaction solution was maintained at 80 °C for 8 h whereupon it was allowed to cool to room temperature and any remaining aggregate particles were removed using a 0.45 μm syringe filter. Eighty millilitres of the colloidal solution were then placed in a Teflon pot with lid in an autoclave (Parr Instruments, UK) and heated and maintained at 220 °C for 12 h. This hydrothermal step was used to grow the particles from 5 to 10–15 nm. Upon removal of the solution from the autoclave the separated out colloidal particles were redispersed using ultrasound. The reaction solution was then concentrated to about 12 wt.% using a rotary evaporator, followed by the addition of 50 wt.% Carbowax 20M to help prevent the formation of small surface cracks when the paste is cast and allowed to dry. The final form of the titanium dioxide paste is a white, mayonnaiselike, substance which appears stable for many months if kept in the fridge. Unless stated otherwise, all titanium dioxide films produced in this work were generated from such a white, titanium dioxide paste and so are referred to as "TiO_2 paste films". Casting the paste to create thick "TiO_2 paste films" involved, typically spreading 0.6 cm^3 of the titanium dioxide paste on the surface of a 25 mm diameter quartz disc mounted on a spin coater and subsequently spinning it at 1000 rpm for 2 s and 2500 rpm for 10 s. The films were then left for approximately 30 min until they changed from white to clear and then calcined in a furnace at 450 °C for 30 min. The average thickness of such films was determined to be 2.7 μm by UV-Vis spectroscopy. X-ray analysis of the titanium dioxide films showed them to be anatase and SEM analysis showed that the films comprised particles typically 13 ± 1 nm in diameter. Previous work showed that such films were largely mesoporous with an average porosity of 60% [9,12].

In order to effect useful comparisons and place the photocatalytic activities of the TiO_2 paste films in context, thin (ca. 43 nm) films of titania were prepared by a traditional sol–gel route [6], using a non-viscous coating solution. In addition, APCVD films of titania on quartz were prepared [10] via a similar route to that associated with Pilkington Glass Activ™ and, finally, samples of Activ™ were obtained from Pilkington Glass [13]. In the preparation of all the above titania-coated samples, with the exception of Activ™, the supporting glass substrates were 2 mm thick, 25 mm diameter, quartz discs. In contrast, the sample of Activ™ comprised a 15 nm thick CVD coating of anatase titania on 4 mm float glass, with a 30 nm thick SiO_2 surface layer to prevent alkali-ion migration. All the above films were tested for photocatalytic activity using stearic acid as the test substrate.

3. Results and discussion

3.1. Spectral features of the prepared films

Typical UV-Vis spectra of all the substrates under test are illustrated in Fig. 1. Thus, from the UV-Vis spectrum of a blank quartz disc (spectrum (a), Fig. 1) it is clear that the underlying substrate is optically clear at all wavelengths >200 nm. The absorption spectrum of a thin (43 nm) titania coating prepared by a traditional sol–gel route, i.e. spectrum (b) in Fig. 1, shows the common spectral characteristics of a titania film [14,15]. Thus, it has a trailing edge to its absorption spectrum in the near-UV which is characteristic of an indirect bandgap semiconductor and a maximum absorbance at ca. 250 nm [15]. Interestingly, the background absorbance of this film, most notable at wavelengths where the semiconductor does not absorb, i.e. >380 nm, is the highest of all the films and is attributed to light scattering. Thus, these films have a slight degree of unwanted haze and so, in our experience, thicker films, prepared by combining this traditional sol–gel route with a number of "coat and bake" cycles, appear much more hazy, as well as fragile, and, therefore, do not offer the optical clarity of the thick (2.7 μm) titania films prepared via the TiO_2 paste method. The UV-Vis spectrum (c), illustrated in Fig. 1, is that for Pilkington Glass Activ™ and a brief comparison of spectra (b) and (c) might tempt the suggestion that Activ™ has a much thicker coating of titania than the 15 nm specified by the manufacturers [16]. However, the very strong absorbance of this material at wavelengths <340 nm is in fact largely due to the supporting 4 mm float glass substrate. At 15 nm thick, the titania coating on Activ™ is expected to absorb very little near-UV light (e.g. $Abs_{365} = 0.033$) and not all far-UV light (e.g. $Abs_{254} = 0.332$) [14]. The collection of UV-Vis spectra identified as (d) in Fig. 1, are those recorded for five different thick-paste TiO_2 films and show that the method of preparation, from the same batch of titania white paste, is highly reproducible. The spectra (d), illustrated in Fig. 1, also show that the thick paste titania films are optically clear, and exhibit a similar clarity to Activ™. Finally spectrum (e) in Fig. 1 illustrates the relative emission spectrum of an 8 W BLB and highlights the significant degree of light absorption that is achieved with thick films of titania (e.g. 58% for the typical 2.7 μm films) and the poor degree of absorption (0.075%) exhibited by thin (43 nm) sol–gel films prepared by a traditional route. Obviously the degree of

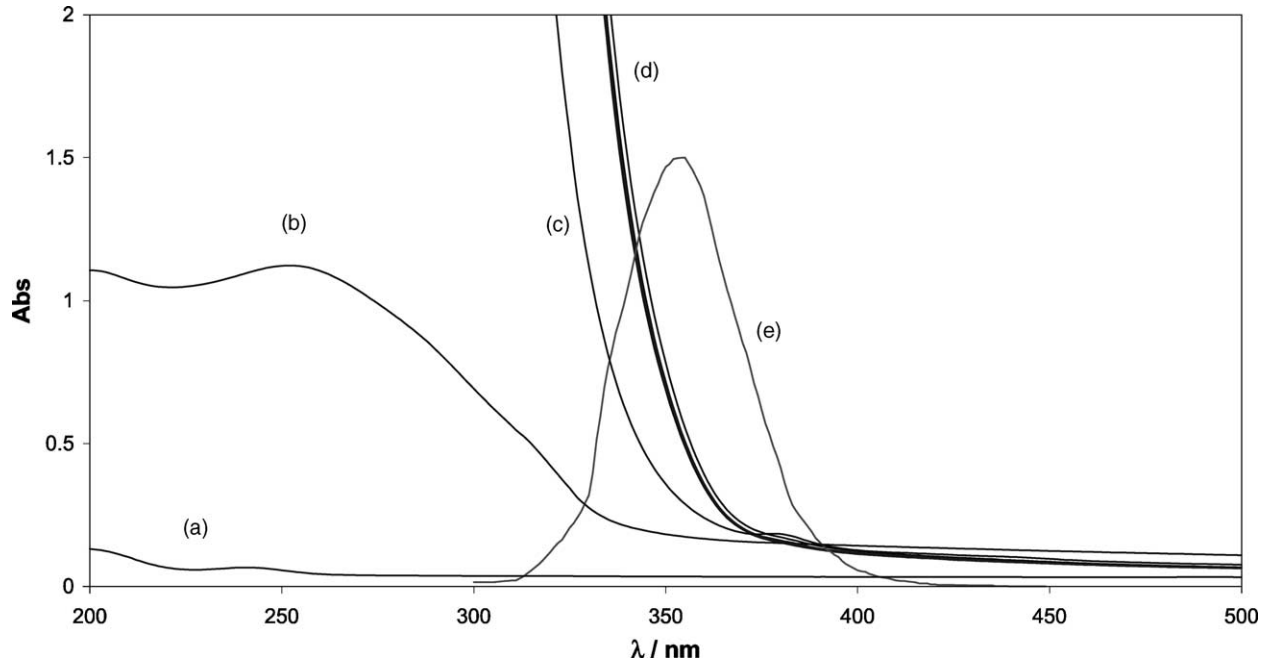

Fig. 1. UV-Vis absorption spectra of (a) 2 mm thick, 25 mm diameter quartz disc, (b) 43 nm titania film produced by a traditional sol–gel method, (c) 4 mm Pilkington Activ™ glass and (d) five thick (2.7 μm) TiO_2 paste films produced from the same batch of white titanium dioxide paste; (e) is the relative emission spectral profile of a 365 nm 8 W BLB.

light absorption by Activ™ (15 nm) will be even lower (ca. 0.026%) than the thin sol–gel films, but this fact is not apparent from the UV-Vis spectrum of Activ™ since, as noted previously, its absorption spectrum is dominated by that of the 4 mm float glass supporting substrate. Several of the optical features discussed above are summarised in Table 1.

3.2. A comparison of photocatalytic activities

A common method used to provide a measure of the photocatalytic activity of a new material involves monitoring the rate of removal of stearic acid [7,8,17–20]. Previous work shows that the removal of stearic acid by semiconductor photocatalysis usually produces no film component, other than stearic acid, that is detectable by FT-IR. This work also shows that no gas products, other than carbon dioxide and water, are generated during the course of the photocatalytic process [18,19]. In addition, research shows that the ratio of the number of moles of stearic acid lost due to the disappearance of stearic acid to the number of moles of carbon dioxide generated at the same time is in the stoichiometric ratio of 1:18 [18]. From the results of this work it appears reasonable

Table 1
Optical and photocatalytic properties of titania-coated glass samples

Film type	Film thickness, d (nm)	Wavelength (absorbance)	Rate, R_i ($\times 10^{13}$ molecules/cm^2/min)	FQE[a] (10^{-4} molecules/photon)	Fraction of light absorbed, f[b]	Quantum yield[c] ($\times 10^{-2}$)
Paste (thick)	2700	254 (>5)	69–105	16–22.9	1	0.16–0.23
Paste (thick)	2700	365	66.0	8.7	0.58	0.15
Paste (thin)	54[d]	254 (1.162)	69.1	15.0	0.93	0.16
Paste (thin)	54[d]	365	15.9	2.1	0.12	0.18
CVD (thin)	52	254 (1.128)	15.3	3.4	0.93	0.04
Activ™	15	254 (0.332)[d]	4.7	1.0	0.53	0.02
Activ™	15	365 (0.0326)[e]	0.6	0.07	0.07	0.01
Traditional sol–gel	43[d]	254 (0.942)	72.8	15.8	0.89	0.18
Traditional sol–gel	43[d]	365	8.8	1.2	0.075	0.16

[a] Formal quantum efficiency [10], δ, calculated as δ = rate of stearic acid destruction (molecules removed/cm^2)/incident light intensity (photons cm^{-2}).

[b] Calculated using $f = (1–10^{-\mathrm{Abs}(\lambda)})$ [14] for 254 nm irradiations or, for 365 nm irradiations, from an analysis of the overlap of the UV-Vis spectra of the film with that of the emission spectrum of the lamp (using the data in Fig. 1). For Activ™ the value of f was calculated from the estimated absorbance of the film at 365 nm; vide infra.

[c] Quantum yield, ϕ, calculated as $\phi = \delta/f$.

[d] Calculated using the formula [14]: $\mathrm{Abs}_\lambda = 0.434\alpha_\lambda d$, the data for Abs_{254} in this table and a value of $\alpha_{254} = (5.1 \pm 0.5) \times 10^5\ \mathrm{cm}^{-1}$.

[e] Calculated using the formula [14]: $\mathrm{Abs}_\lambda = 0.434\alpha_\lambda d$, a given film thickness of 15 nm and a value of $\alpha_{365} = (0.5 \pm 0.5) \times 10^5\ \mathrm{cm}^{-1}$.

to assume that the kinetics of the disappearance of stearic acid, as measured by the FT-IR method employed in this work, for example, is also a direct measure of the kinetics of the photocatalytic destruction of stearic acid; the overall process which may be summarised as follows [7,17–20]:

$$C_{17}H_{35}COOH + 26O_2 \overset{TiO_2, h\nu}{\rightarrow} 18CO_2 + 18H_2O \quad (3)$$

As this process involves the transfer of 104 electrons it would appear likely that the maximum quantum yield for this process should be 1/104, i.e. about 0.01.

Using transmission FT-IR spectroscopy it was possible to measure the rates of stearic acid photocatalytic destruction sensitised by the various titania films under test using both blacklight bulbs and germicidal lamps as the irradiation sources. The results of this work are given in Table 1 and show that the thick paste titanium dioxide films exhibit a similar rate, and formal quantum efficiency (FQE) [10], for the destruction of stearic acid using either near-UV or far-UV light. In contrast, thin titanium dioxide films, made either using a diluted form of the paste or using a traditional sol–gel method, exhibited very low FQEs for stearic acid removal using near-UV light, but were much more efficient when far-UV light was used instead. The difference in rate, and FQE, exhibited by traditional (thin) sol–gel films, and thin paste films for that matter, is mainly due to the different extent that the film is able to absorb near-UV (ca. 7.5%) and far-UV (ca. 89%) light. Such differences are eliminated if the quantum yields, rather than FQE's are calculated. Indeed, what is striking about all the sol–gel films tested, including the traditional sol–gel and thin TiO_2 paste films, is the very similar value for the quantum yield for the destruction of stearic acid, i.e. typically 0.16%, at excitation wavelengths of either 365 and 254 nm (see Table 1). Interestingly, titania coated by an APCVD method onto quartz or Pilkington Glass Activ™ (also prepared by an APCVD method but onto 4 mm float glass) exhibited a significantly lower quantum yield for the photocatalytic removal of stearic acid compared with that for any of the sol–gel films tested. The reasons for this striking difference in photocatalytic activity are not clear, but may be due to porosity, since it is known that the sol–gel films are highly porous [9] whereas, from SEM imaging, the APCVD titania films appear much more compact [10]. The results in Table 1 show that thick titanium dioxide films are able to utilise near-UV light for the photocatalytic destruction of stearic acid far more efficiently than thin titanium dioxide films produced by the traditional sol–gel route, or by APCVD methods. From the results in Fig. 1 it is also clear that such thick films exhibit a high degree of optical clarity and therefore appear attractive as a coating for glass. These thick TiO_2 paste films are reasonably robust and are resistant to damage by the 3M Scotch Tape™ test and abrasion by pencils with a hardness up to HB [7]. In the following section the photocatalytic removal of stearic acid by these thick TiO_2 paste films is examined in more detail.

3.3. Kinetics of photocatalysis

The kinetics of the photocatalytic destruction of stearic acid, via reaction (3), were studied as a function of initial stearic acid concentration, over the range: $(1.2–5.6) \times 10^{16}$ molecules of stearic acid cm^{-2}, which can be shown to be equivalent to a stearic acid layer thickness range of 64–300 nm [21]. Some of the [stearic acid] versus irradiation time decay profiles did show some evidence of a tail to the decay profiles, particularly at high stearic acid levels, as illustrated in Fig. 2. This latter feature may be due to the accumulation of a small amount of material that is more difficult to destroy, as suggested by others [18]. However, for the most part, the rate of decay appeared largely independent of the stearic acid concentration as illustrated by the results in Fig. 2, and a plot of the initial rate versus [stearic acid], illustrated in the insert diagram of Fig. 2. Such zero-order kinetics for reaction (3) have been reported by others in similar studies and are usually attributed to the complete coverage of the titania photocatalyic active sites by the stearic acid [7,18]. This appears a likely situation in this work given that the initial stearic acid concentrations employed corresponded to 26–120 monolayers of the substance.

3.4. Reproducibility and repeatability

As noted above, five thick (2.7 μm) paste films were prepared. From their UV-Vis (spectra (d) in Fig. 1), they appeared optically very similar. Their photocatalytic activities, under near-UV irradiation, were also tested and the observed variations in the integrated areas under the stearic acid FT-IR peaks as a function of irradiation time are illustrated in Fig. 3. From the results of this work it appears that the photocatalytic ability of each of these five films to destroy stearic acid via reaction (3) is very similar. Indeed a plot of initial rate versus sample number, illustrated in the insert diagram of Fig. 3, reveals an average rate (0.21 Abs units $min^{-1} \equiv 6.6 \times 10^{14}$ molecules of stearic acid cm^{-2}) that is largely independent of the sample number. Thus, thick TiO_2 paste titania films produced from the same batch of TiO_2 paste appears to produce very reproducible films. Typically these films exhibited a quantum yield for reaction (3) of 0.15% (see Table 1). However, more recent work, carried out using different batches of the titania paste revealed some batch-to-batch variation in activity; with some batches reaching quantum yields up to 0.23% (see Table 1). This variation appears largely due to the age of the paste, with freshly made pastes appearing slightly more active than ones that have been stored for some time. Presumably this difference in photocatalytic activity is due to a slow particle aggregation process, with older films, comprised of slightly larger particles, exhibiting a diminished effective surface area for photocatalysis and, therefore, a reduced photocatalytic activity and quantum yield.

The elegant work of Pichat and co-workers [22] in the early 1990s established that the same sample of titania, such

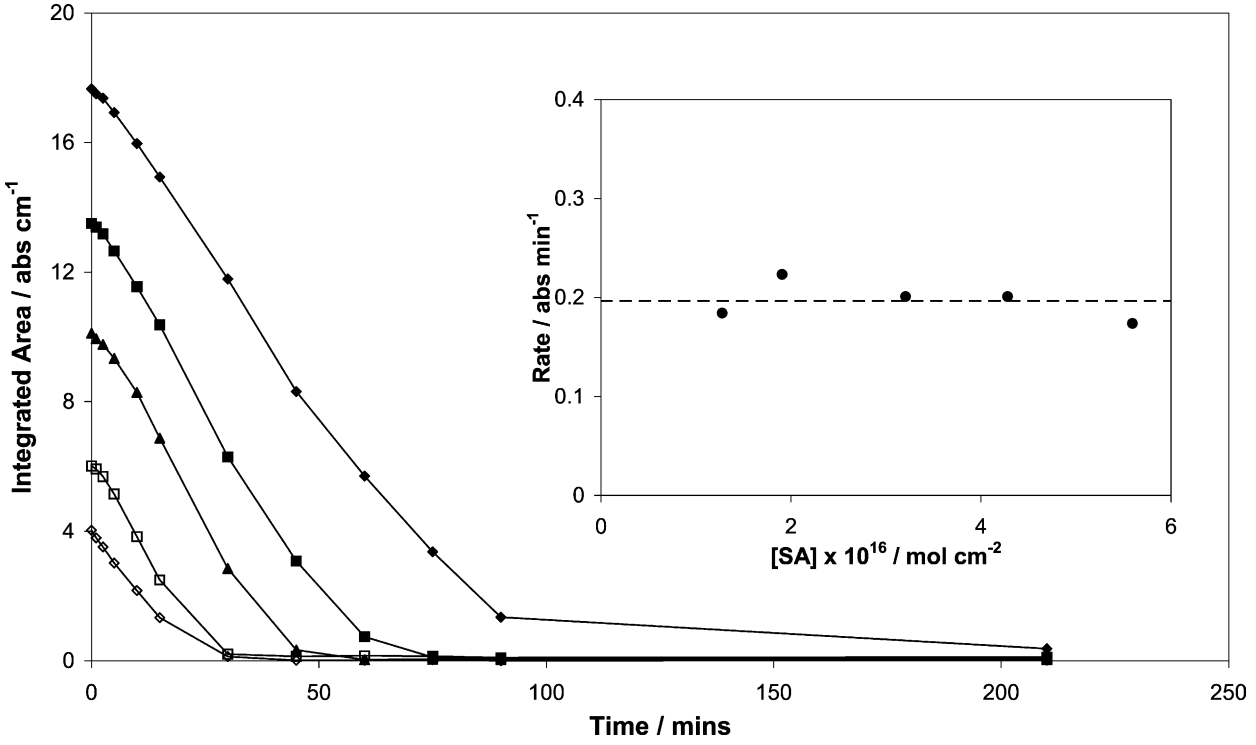

Fig. 2. Kinetics: plot of a series of profiles of the integrated area under the stearic acid peaks, as measured by FT-IR, as a function of irradiation time, using six 8 W BLBs as the irradiation source. Each profile corresponds to a different initial amount of stearic acid, but the same thick TiO_2 paste film was used throughout. The insert diagram is a plot of the initial rate (taken from the data in the main diagram) as a function of initial stearic acid concentration (as determined from the measured initial integrated area).

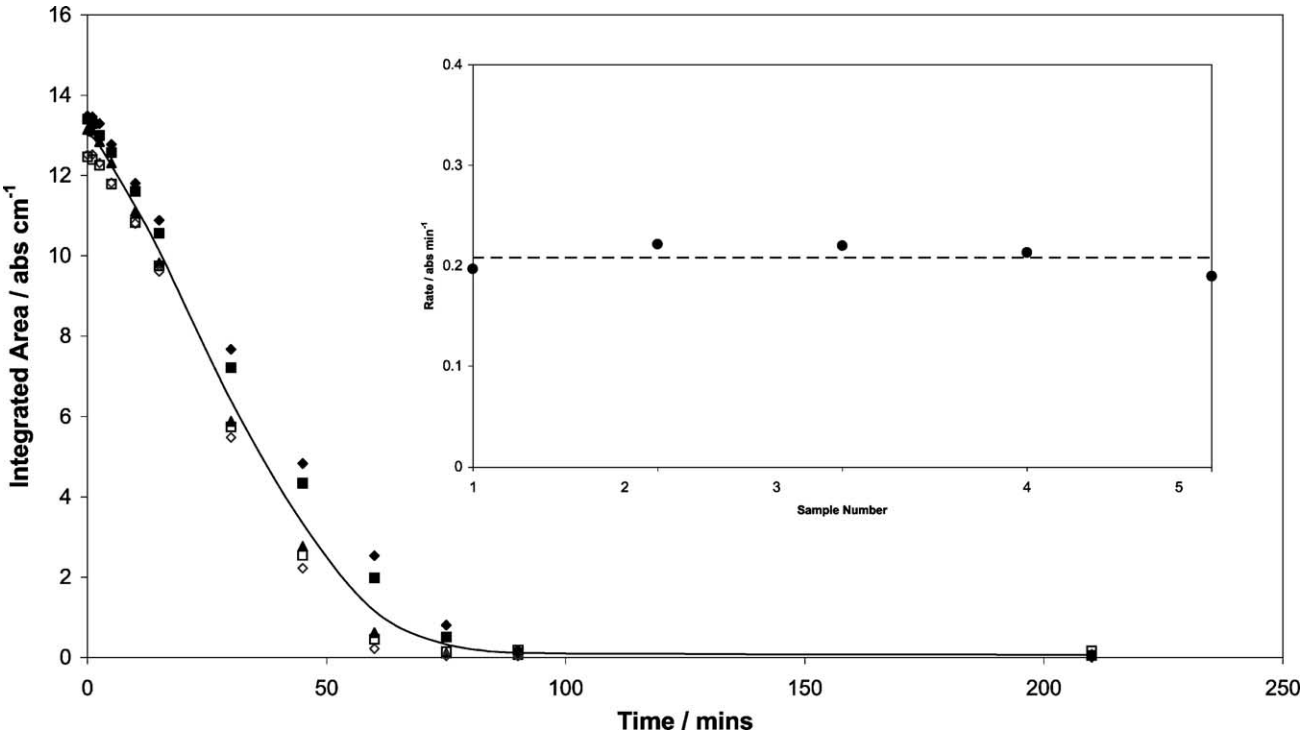

Fig. 3. Reproducibility: plot of a series of profiles of the integrated area under the stearic acid peaks as a function of irradiation time, using six 8 W BLBs as the irradiation source. Each profile corresponds to a different thick TiO_2 paste film, made from the same batch of white paste in an identical manner. For each film tested the initial stearic acid concentration was kept the same. The insert diagram is a plot of the initial rate (taken from the data in the main diagram) as a function of film sample number.

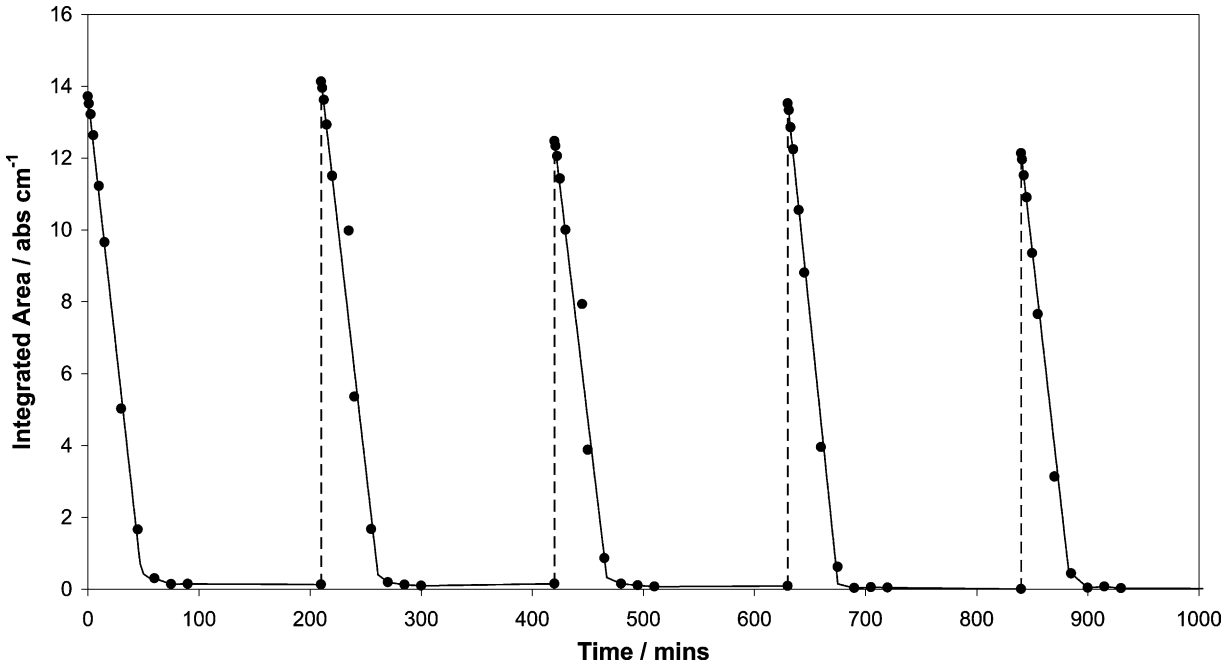

Fig. 4. Repeatability: plot of a profile of the integrated area under the stearic acid peaks as a function of irradiation time, using six 8 W BLBs as the irradiation source. The series of decay profiles were recorded using the same thick TiO_2 paste film. The broken lines indicate the point of addition of a further amount of stearic acid after the complete removal of the last one.

as Degussa P25, is able to photocatalyse the destruction of an organic test pollutant (such as 4-chlorophenol) repeatedly without exhibiting any evidence of wear, poisoning or photoaging. Encouragingly, as illustrated by the results in Fig. 4, thick paste titania films appear able to mediate the photodestruction of stearic acid, via reaction (3), many times without exhibiting any evidence of activity loss. It can be shown that an integrated area under the stearic acid peaks of 14 cm^{-1} is equivalent to a stearic acid layer comprising 95 monolayers and is ca. 0.238 μm thick [21], since a monolayer of stearic acid is ca. 2.5 nm [17]. Thus, from the results of the repeatability study illustrated in Fig. 4, since the typical initial integrated stearic acid area is ca. 13 cm^{-1}, it follows that after five cycles the thick paste film has removed ca. 1.1 μm of stearic acid in ca. 250 min of irradiation time, i.e. at a rate of ca. 4.4 nm min^{-1} and a thickness equivalent to ca. 40% of the thickness of the TiO_2 paste film. Blank experiments show that no stearic acid is removed under the same irradiation conditions, if the titania photocatalyst film is absent.

3.5. Light intensity effects

A series of titania paste films of different thickness on quartz were prepared by using different spin speeds and dilutions of the original paste. The UV-Vis absorption spectra of these different films are illustrated in Fig. 5 and show that all the films have a similar spectral shape and have effective absorbances at 254 nm that span the range 0.077–1.327. It follows from this data that their thicknesses span the range 3.6–61.4 nm, given $Abs_\lambda = 0.434\alpha_\lambda d$, where α_λ is the absorption coefficient of titania at wavelength λ ($\alpha_{254} = 5.1 \times 10^5\ cm^{-1}$) and d is the film thickness (cm) [14]. The initial rates of destruction of stearic acid via reaction (3) using far-UV, 254 nm, light were determined for each of the titania paste films of different thickness and the results plotted as a function of fraction of light absorbed at 254 nm, i.e. $f_{254}(= 1–10^{-Abs(254)})$ [14], as illustrated in the insert diagram in Fig. 5. The latter plot appears a good straight line indicating that the rate of photoreaction (3) is directly proportional to absorbed light intensity. Many studies of a variety of different photocatalytic reactions of the sort summarised by reaction (1), sensitised by titania, reveal that the overall rates of reaction are proportional to absorbed light intensity (I_{Abs}) at low absorbed light levels [1,23,24]. In contrast, at high absorbed light intensities it is usually found that the rates of such reactions are proportional to $I_{Abs}^{1/2}$, thus indicating that electron–hole recombination is the dominant process [1,23,24]. Since in this work the initial rate of reaction (3) is proportional to I_{Abs}, it is possible to estimate, from the gradient (=0.33 Abs min^{-1}) of the line of best fit to the data in the insert diagram in Fig. 5, an overall quantum yield for the process of 0.23%, given that the incident light intensity was 4.6×10^{17} photons cm^{-2} min^{-1}. This value for the quantum yield differs slight from the average value reported earlier of 0.15% and which appeared common to all the sol–gel films tested. However, as noted earlier, the enhanced value of 0.23% is attributed the freshness of the titania paste used to make the films used in this part of the work.

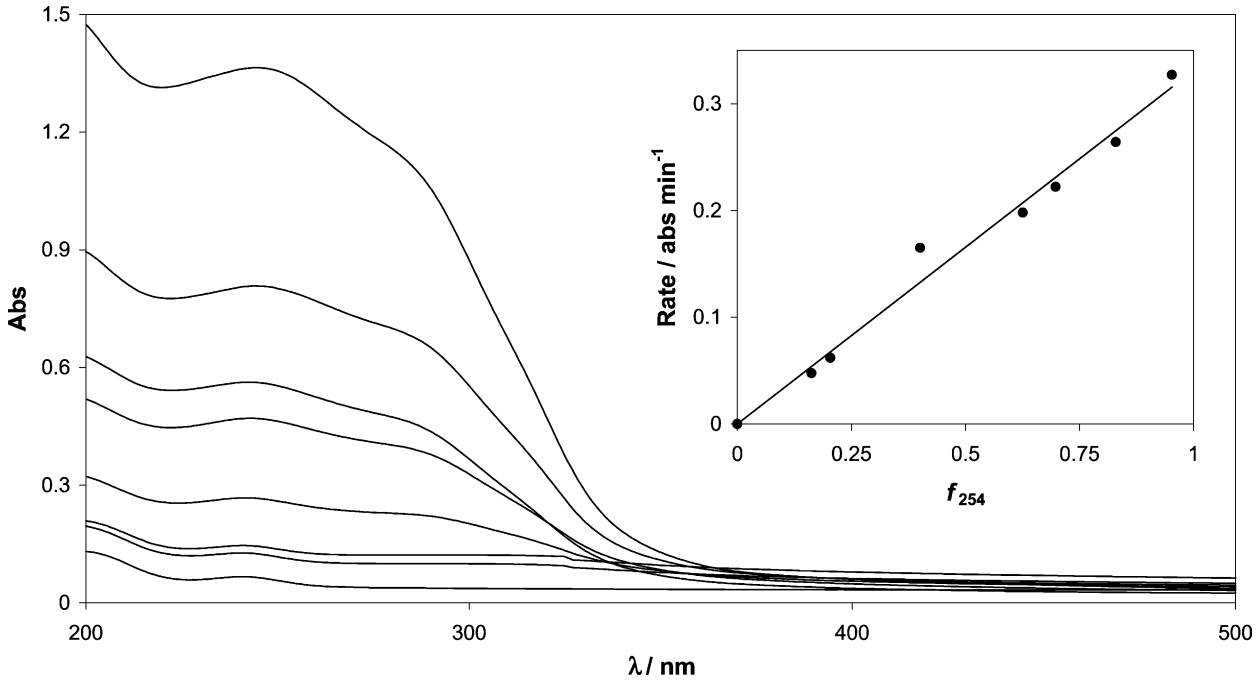

Fig. 5. UV-Vis spectra of a series of thin (3.6–61.4 nm) TiO_2 paste films prepared by using a combination of different spin coating speeds and diluting the original white titania paste. The insert diagram is a plot of the measured rate of removal of stearic acid as a function of the fraction of 254 nm light absorbed, f_{254}. In this work six 8 W germicidal lamps were used as the irradiation source.

A similar direct relationship between initial rate and absorbed light intensity, was found when near-UV (BLB) light was used. The latter observation is not too surprising given that such a relationship is expected at low absorbed light intensities and the I_{Abs} values for the near UV study were much less than those for the far UV study. Thus, although the near-UV incident light intensity from the six BLBs was 65% greater than that used in the far-UV study (see Section 2), the absorbances (and therefore, degree of light absorption) of the films were significantly less in the near-UV, compared to the far-UV.

3.6. Rate as a function of temperature

The kinetics of reaction (3) were studied briefly as a function of temperature, over the range 20–40 °C. An Arrhenium plot of the initial rate as a function of temperature, i.e. $\ln(r_i)$ versus T^{-1}, revealed an overall activation energy of 2.5 kJ mol^{-1}. This low activation energy appears in line with the findings of others who have reported, for reaction (1) sensitised by titania, values ranging from +17 to −15 kJ mol^{-1} [25]. An activation energy of 2.5 kJ mol^{-1} is near to the zero value expected if the overall rate of reaction (3) depends simply upon the rate of generation of electron–hole pairs.

3.7. Photoinduced superhydrophilicity

The profiles of a typical water droplet on the surface of thick TiO_2 paste film before and after ultra-bandgap irradiation are illustrated in Fig. 6. From these results it appears that the porous nature of the films renders their surfaces reasonably hydrophilic, without UV illumination. Thus, for a typical initial, i.e. non-irradiated, TiO_2 paste film the water droplet contact angle is ca. 25°, which is low compared to plain glass (ca. 40°) and non-irradiated traditional sol–gel, (55°) Activ^{TM} (67°) titania films. Degussa P25 films on glass, although very fragile, are also exceedingly porous and thus exhibit an even lower initial water droplet contact angle (8°) [10]. The surface of a thick TiO_2 paste film is rendered highly hydrophilic upon ultra-bandgap illumination, as illustrated by the associated water droplet profile illustrated in Fig. 6. Indeed, all titania films tested exhibited the feature of photoinduced hydrophilicity, so that after prolonged (60 min, two 8 W germicidal lamps) UV irradiation all had water droplet contact angles of 0°. The CVD and Activ^{TM} films appeared to take a little longer than the sol–gel films to reach this superhydrophilic state. All films could be returned to their initial, more hydrophobic state, without any apparent detriment to their photocatalytic or PSH properties, upon subjection to ultrasound, from a ultrasound bath, for 6 min [26].

The variation of the water droplet contact angle on the surface of a thick paste TiO_2 film as a function of ultra-bandgap irradiation time was determined and the results are illustrated in Fig. 7. From these results it appears that the thick TiO_2 paste film exhibits the typical hyperbolic dependence of contact angle with irradiation time that has been observed by others for 240 nm thick films produced by a traditional

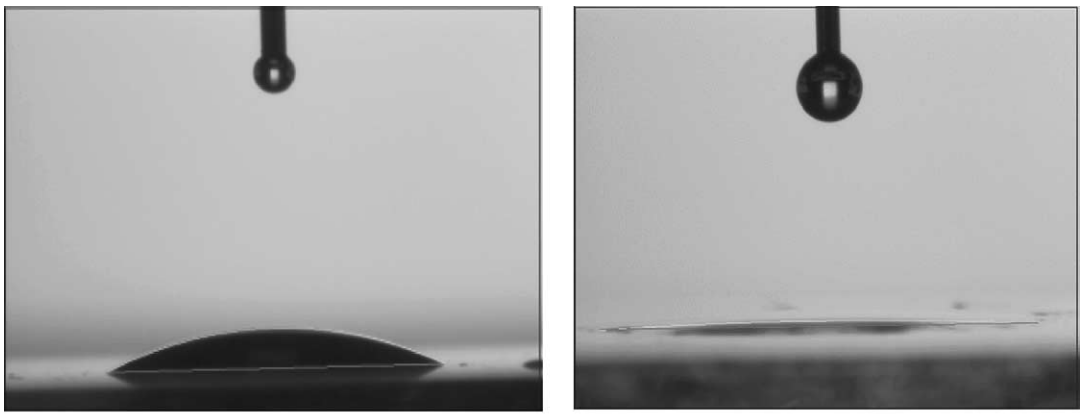

Fig. 6. CCTV images of a water droplet, 30 s after its initial deposition, on the surface of a thick TiO_2 paste film (a) before and (b) after 30 min irradiation with two 8 W germicidal lamps.

sol–gel route [5]. Note: three "coat and bake" cycles were needed to produce these films. The latter workers produce evidence that the reciprocal of the contract angle corresponds to the density of the sites for surface hydroxyl groups reconstructed by UV irradiation [5]. A plot of the results illustrated in Fig. 7 in the form of the reciprocal of the contact angle versus irradiation time generates a good straight line of gradient (k_2 (see reaction (2)) $= 0.012\,\mathrm{deg}^{-1}\,\mathrm{min}^{-1}$) which are typical of those observed by others for titania films at low absorbed light intensities [5].

In contrast to the light-driven, forward process of PSH, i.e. reaction (2), the kinetics of the dark recovery of the water contact angle with time appear biphasic, as illustrated by the results for a typical thick TiO_2 paste in the insert diagram of Fig. 7. Once again the observed behaviour for these thick titania films appears similar to that reported by other

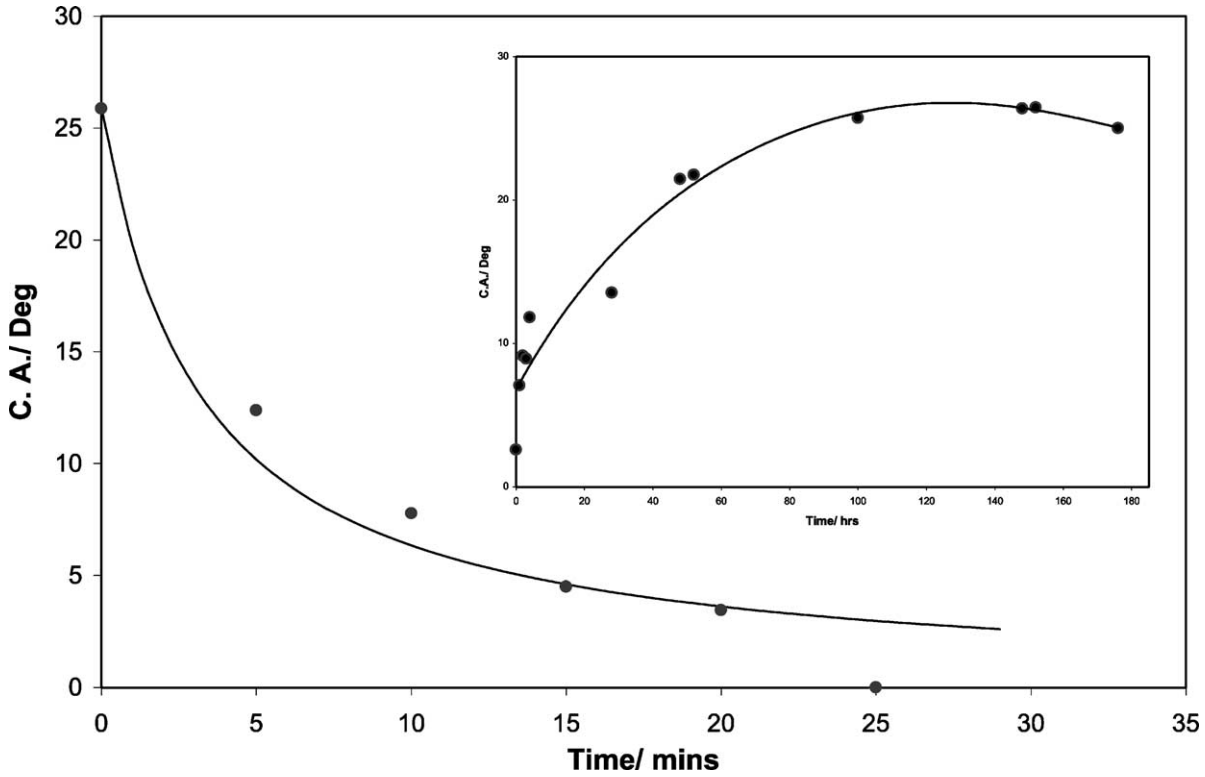

Fig. 7. Plot of the measured variation in contact angle (°) as a function of irradiation time for a thick TiO_2 paste film. The solid line is a line of best fit based on a hyperbolic decay profile. The insert diagram illustrates the recovery in contact angle as a function of time left in the dark.

for thinner (240 nm) titania films produced by a traditional sol–gel route [5]. Indeed, the latter workers note that a plot of the reciprocal of the contact angle recovery data for a traditional sol–gel film as a logarithm of the dark time gives a reasonable straight line (gradient = 0.00744) and so it does with our films (gradient = 0.0426). The difference in the two gradients reflects the difference in recovery rates with the traditional sol–gel films taking >35 days to recover [5], whereas the TiO_2 paste films recover within ca. 5 days. There appears at present no reasonable mechanism to explain why the change of the reciprocal of the contact angle of either thick or thin titania films varies proportionally as a function of the logarithm of the dark time. Indeed, as an alternative, this dark process appears to be also quite well described as a biphasic process with an initial fast step followed by a slower second step. Certainly a plot of the reciprocal of the contact angle versus dark time for the thick TiO_2 paste films yields what appears to be a reasonable combination of two straight lines in series describing a fast ($k_{-2} = -0.064\,\mathrm{deg}^{-1}\,\mathrm{h}^{-1}$) followed by a slow ($k^*_{-2} = -0.0004\,\mathrm{deg}^{-1}\,\mathrm{h}^{-1}$) step in the recovery process. Only further work and a greater understanding of the PSH phenomenon will reveal which, if any, of the above two relationships are mechanistically appropriate in describing the kinetics of the reverse process in reaction (2).

4. Conclusion

Thick paste TiO_2 films are effective photocatalysts for the destruction of stearic acid using near or far UV. The quantum yield for this process is typically 0.15%, although some batches of paste yielded films with quantum yields of up to 0.23%. These quantum yields are significantly greater (4–8-fold) than those found for titania films produced by an APCVD technique, including the commercial self-cleaning glass product Activ^{TM}. As photocatalysts for the destruction of stearic acid the films are reproducible, do not show any evidence of photoaging or wear and are mechanically robust and optically clear. The kinetics of stearic acid destruction are zero order with an activation energy of ca. $2.5\,\mathrm{kJ\,mol}^{-1}$. All titania films tested, i.e. sol–gel and APCVD, exhibited PSH. The light-induced fall, and dark recovery, in the contact angle of titania paste films are similar in profile to those described by others for thin titania films produced by a traditional sol–gel route [5].

Acknowledgements

AM thanks the EPSRC for grant GR/M95042/01 and Pilkington Glass for samples of Activ^{TM}. IPP and SON thank the EPSRC for grant GR/M95059.

References

[1] A. Mills, S. LeHunte, J. Photochem. Photobiol. A 108 (1997) 1.
[2] A. Fujishima, T.N. Rao, D. Tryk, Titanium dioxide photocatalysis, J. Photochem. Photobiol. C 1 (2000) 1.
[3] A. Mills, S.-K. Lee, J. Photochem. Photobiol. A 152 (2002) 233.
[4] R. Wang, K. Hashimoto, A. Fujishima, M. Chikuni, E. Kojima, A. Kitamura, M. Shimohigoshi, T. Watanabe, Nature 388 (1997) 431.
[5] N. Sakai, A. Fujishama, T. Watanabe, K. Hashimoto, J. Phys. Chem. B 107 (2003) 1028.
[6] N. Negishi, T. Iyoda, K. Hashimoto, A. Fujishima, Chem. Lett. (1995) 841.
[7] Y. Paz, Z. Luo, L. Rabenberg, A. Heller, J. Mater. Res. 10 (1995) 2842.
[8] R. Fretwell, P. Douglas, J. Photochem. Photobiol. A 143 (2001) 229.
[9] A. Mills, N. Elliott, G. Hill, D. Fallis, J.R. Durrant, R.L. Willis, Photochem. Photobiol. Sci. 2 (2003) 591.
[10] A. Mills, N. Elliott, I.P. Parkin, S.A. O'Neill, R.J. Clark, J. Photochem. Photobiol. A 151 (2002) 171.
[11] J.G. Calvert, J.N. Pitts, Photochemistry, Wiley, New York, 1967, p. 783.
[12] C.J. Barbé, F. Arendse, P. Comte, M. Jirousek, F. Lenzmann, V. Shklover, M. Grätzel, J. Am. Ceram. Soc. 80 (1997) 3157.
[13] D.W. Sheel, R.J. McCurdy, S.J. Hurst, Patent Application WO 98/06675, 1998.
[14] A. Mills, S.-K. Lee, A. Lepre, I.P. Parkin, S.A. O'Neill, Photochem. Photobiol. Sci. 1 (2002) 865.
[15] A. Hagfeldt, M. Graetzel, Chem. Rev. 95 (1995) 49.
[16] K.D. Sanderson, A. Mills, I.P. Parkin, S. Hurst, A. Lepre, T. McKittrick, D. Rimmer, L. Ye, Proceedings of the 46th Annual Conference on Society of Vacuum Coaters, 2003, p. 1.
[17] P. Sawunyama, L. Jiang, A. Fujishima, K. Hashimoto, J. Phys. Chem. B 101 (1997) 11003.
[18] T. Minabe, D.A. Tryk, P. Sawunyama, Y. Kikuchi, K. Hashimoto, A. Fujishima, J. Photochem. Photobiol. A 137 (2000) 53.
[19] S. Sitkiewitz, A. Heller, New J. Chem. 20 (1996) 233.
[20] T. Watanabe, T. Takizawa, K. Honda, J. Phys. Chem. 81 (1977) 1845.
[21] A. Mills, A. Lepre, N. Elliott, S. Bhopal, I.P. Parkin, S.A. O'Neill, J. Photochem. Photobiol. A, accepted for publication.
[22] G. Al-Sayyed, J.C. D'Oliveira, P. Pichat, J. Photochem. Photobiol. A 58 (1991) 99.
[23] C.S. Turchi, D.F. Ollis, J. Catal. 122 (1990) 178.
[24] T.A. Egerton, C.J. King, J. Oil Col. Chem. Assoc. 62 (1979) 386.
[25] A. Mills, R. Davies, J. Photochem. Photobiol. A 85 (1995) 173.
[26] N. Sakai, R. Wong, A. Fujishima, T. Watanabe, K. Hashimoto, Langmuir 14 (1998) 5918.